Volume 38 | Number 5 | May 2014 | Pages 1811–2146

NJC

New Journal of Chemistry

A journal for new directions in chemistry

www.rsc.org/njc

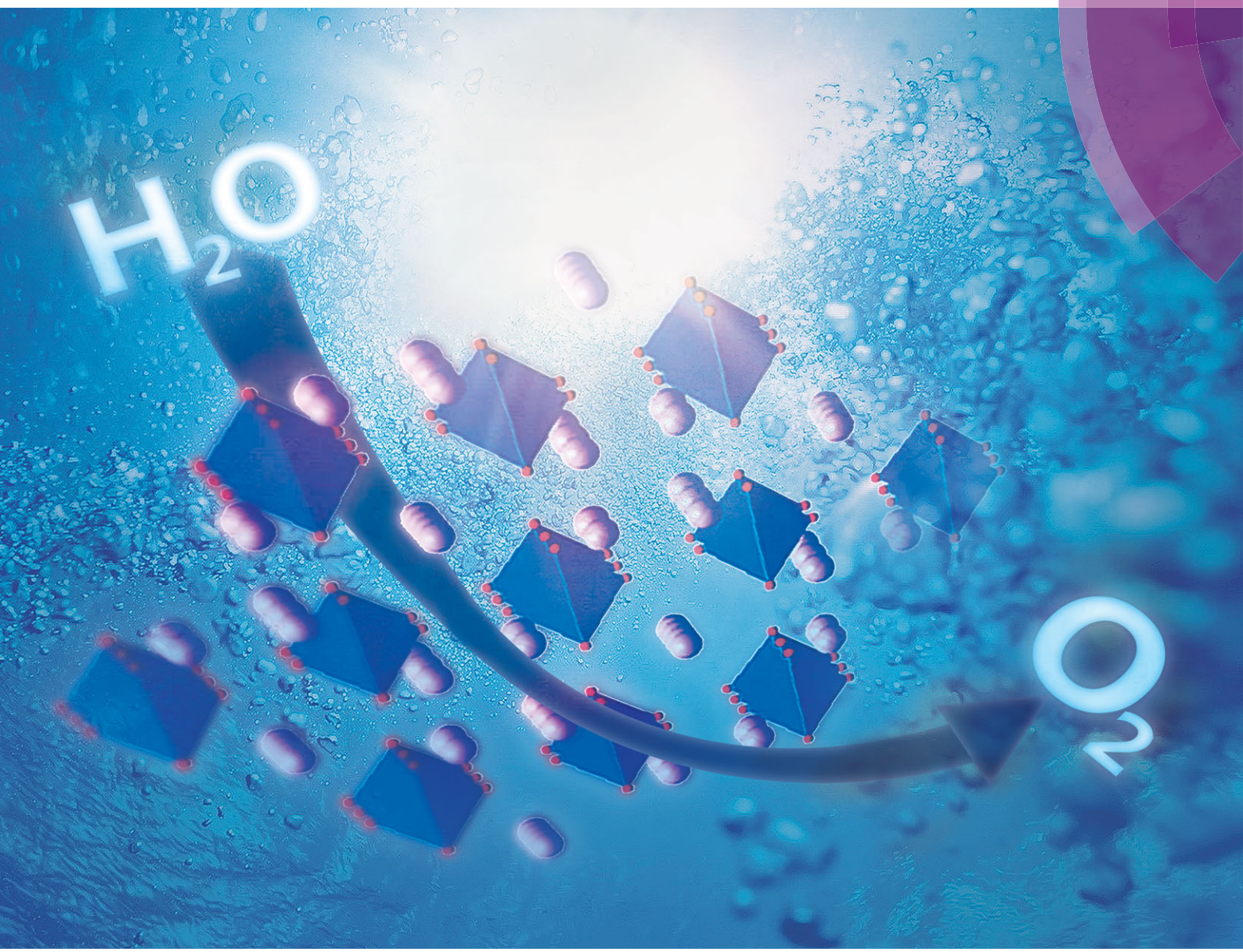

ISSN 1144-0546

ROYAL SOCIETY OF CHEMISTRY

LETTER

Matthias Driess *et al.*

Visible light driven non-sacrificial water oxidation and dye degradation with silver phosphates: multi-faceted morphology matters

cnrs

NJC

LETTER

View Article Online
View Journal | View Issue

Visible light driven non-sacrificial water oxidation and dye degradation with silver phosphates: multi-faceted morphology matters†

Cite this: *New J. Chem.*, 2014, 38, 1942

Received (in Montpellier, France) 27th August 2013,
Accepted 16th October 2013

DOI: 10.1039/c3nj01012k

www.rsc.org/njc

Arindam Indra, Prashanth W. Menezes, Michael Schwarze and Matthias Driess*

The convenient synthesis of multi-faceted *versus* irregular shaped Ag_3PO_4 microparticles for the visible light driven non-sacrificial water oxidation is reported. Strikingly, the multi-faceted particles are found to be more effective for oxygen evolution reaction (OER) by photocatalytic water oxidation in water and in phosphate buffer solutions as well as for dye degradation in comparison to the irregular shaped particles.

Increasing demand for global energy production and reducing the amount of greenhouse gases need to find an alternative source of energy.[1] In nature, photosynthesis is the most efficient system for the conversion of solar to chemical energy.[2] Artificial photosynthesis with visible light is a widely studied area of research for the alternative source of energy production. Considerable attempts have been already made to develop the structural and functional mimics of photosystem II (PS II) for the effective water splitting but the respective results are still far from the level of operation.[3] Since calcium and manganese exist at the cores of PS II, numerous heterogeneous manganese oxides and calcium manganese oxide based catalysts have been synthesized and explored for biomimetic water oxidation.[4]

Another functional approach for overall water splitting is to apply a semiconducting photocatalyst with suitable band gaps and band positions.[5] Photo-excited electron–hole pairs were separated at the semiconductor catalyst surface where the electrons reduce protons to generate hydrogen while the holes oxidize water to evolve dioxygen molecules. Migration of electrons and holes to the surface by hindering their recombination is the most crucial step to control the overall process. Design of such an appropriate semiconductor with all the aforesaid criteria is difficult to achieve and therefore, often combination of two materials has been used to enable overall water splitting. This reaction is indeed considered as the two coupled half reactions that generate hydrogen and oxygen from water.[6] However, oxidation of water to oxygen is regarded as the bottleneck of the overall water splitting process as it involves four electrons and four protons transfer with the thermodynamic and kinetic limitations.[7]

Several photocatalysts have been investigated for the photochemical and photoelectrochemical water oxidation reactions.[8] In fact, the metal ion doped, substituted or intercalated titanium oxides, tantalum oxides, niobium oxides are proven to be extremely active for the visible light driven water oxidation.[9] Successful efforts leading to control and alteration of the band gaps by substituting the oxygen atoms of the metal oxide with heteroatoms (nitrogen or sulphur) have been made and were found to be very effective.[10] Recent developments demonstrated that tungsten oxide (WO_3) can act as a suitable oxygen evolution reaction (OER) catalyst in the visible region in the presence of a co-catalyst and a sacrificial agent.[11] Bismuth vanadate ($BiVO_4$)[12] and ferric oxide (Fe_2O_3)[13] photoanodes for the water splitting under visible light irradiation were also extensively studied.

Silver phosphate (Ag_3PO_4) has a band gap of 2.4 eV and can absorb visible light. Interestingly, its band edge values are more positive than the oxidation potential of water, making it a potential candidate for water oxidation.[14] Photochemical water oxidation with Ag_3PO_4 in the presence of silver nitrate ($AgNO_3$) as the sacrificial electron acceptor was first reported by Yi *et al.*[15] Nevertheless, for the overall water splitting, the OER half reaction should be performed in the absence of any sacrificial agent.

Ag_3PO_4 is also well known to show degradation of dye under visible light irradiation.[16] Lately, Ye *et al.* described that enhanced catalytic activity for the dye degradation was due to the sharp corner and edges of silver phosphate of submicron-structured cubes.[16] Superior photocatalytic performance for the degradation of Rhodamin B dye was achieved with concave trisoctahedral Ag_3PO_4 with high-index facets.[17] It was reported that rhombic dodecahedron microcrystals of Ag_3PO_4 show better photocatalytic activity than cubic microcrystals for the dye degradation under visible light irradiation.[18]

Department of Chemistry, Metalorganics and Inorganic Materials, Technische Universität Berlin, Strasse des 17 Juni 135, D-10623 Berlin, Germany. E-mail: matthias.driess@.tu-berlin.de

† Electronic supplementary information (ESI) available: Experimental procedures, PXRD, EDX analysis and other figures. See DOI: 10.1039/c3nj01012k

For both, the OER and the dye degradation, as the catalytic activity of Ag_3PO_4 increases, photocorrosion of the catalyst becomes unavoidable. Therefore, it is challenging to change the synthetic protocol to prepare Ag_3PO_4 with novel morphology that could enhance the catalytic activity with increased photostability.

Herein, we report the synthesis of Ag_3PO_4 nanoparticles with multi-faceted *vs.* irregular morphology. The latter materials were studied both for the photochemical OER in the absence of any sacrificial agent in water (pH = 7) as well as in phosphate buffers (pH = 1–10). Comparison of the catalytic performance of the newly synthesized material with other well known WO_3 and $BiVO_4$ photocatalysts revealed that only Ag_3PO_4 was efficient in non-sacrificial water oxidation whereas negligible amounts of oxygen were produced with other two photocatalysts. Degradation of organic dye Methyl Blue (MB) was also achieved in a faster rate for multi-faceted Ag_3PO_4 than the irregular shaped ones.

Ag_3PO_4(1) nanoparticles were synthesized in water-in-oil emulsion by the reaction of $AgNO_3$ and phosphoric acid (see Experimental and Scheme 1). Ag_3PO_4(2) was synthesized by the stoichiometric reaction of Na_2HPO_4 (48 mg) and $AgNO_3$ (169 mg) in 10 mL of water at room temperature. For the comparison of photocatalytic activity under non-sacrificial conditions, $BiVO_4$ was prepared by the literature reported procedure[19] while WO_3 was purchased from Sigma-Aldrich.

SEM images of Ag_3PO_4(1) show multi-faceted particles with the size of 600–700 nm. The particle faces are mostly smooth and have sharp edges (Fig. 1a). For Ag_3PO_4(2), smaller irregular shaped particles forming a layered structure were observed (Fig. 1b). Obviously, the synthesis of Ag_3PO_4(1) microparticles in the presence of oleic acid and water-in-oil emulsion helps in building the multi-faceted morphology with sharp edges. The EDX spectrum of Ag_3PO_4(1) confirmed the presence of Ag, P and O as the only elements (Fig. S1, ESI†).

Reflections obtained from the powder X-ray diffraction (PXRD) patterns revealed that both synthesized Ag_3PO_4 crystallise in the body centered cubic (bcc) structure as shown in Fig. 2 and Fig. S2 (ESI†).[20] The crystal structure of Ag_3PO_4 comprises of a phosphate tetrahedron sharing its corners with four oxygen atoms (Fig. 2, inset). The lattice parameters (a = 6.004 Å) of Ag_3PO_4(1) and Ag_3PO_4(2) are in accordance with the previously reported cubic structure (JCPDS 70-702). Diffuse reflectance spectra of both Ag_3PO_4 displayed strong absorbance starting at 520 nm (Fig. 3). Band gaps of the synthesized photocatalysts were determined using the Kubelka–Munk equation: $(\alpha h\nu)^{1/2} = A(h\nu - E_g)$ where α, ν, A, and E_g are the absorption coefficient, light frequency, proportionality constant and band gap, respectively. Extrapolating the plot of $(\alpha h\nu)^{1/2}$ *vs.* $h\nu$, the band gap was

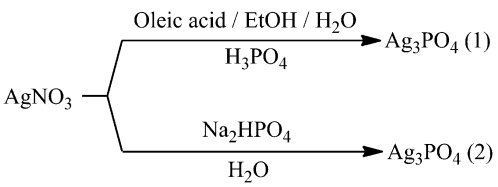

Scheme 1 Synthetic routes for the preparation of the multi-faceted *vs.* irregular shaped silver phosphate microparticles.

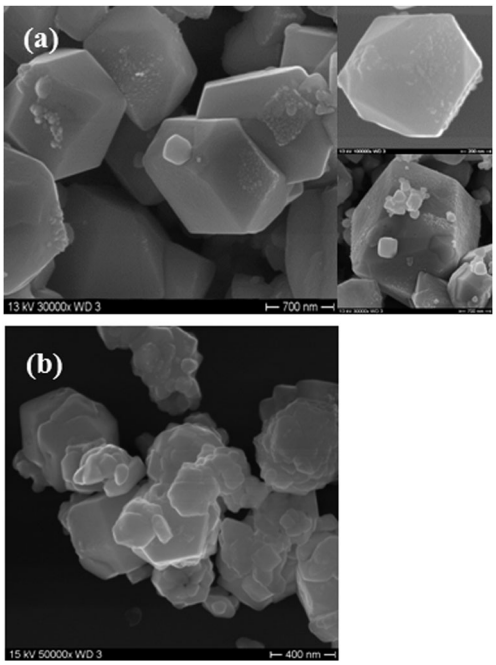

Fig. 1 SEM images of (a) multi-faceted Ag_3PO_4(1), inset showing a single particle from two different directions and (b) irregular shaped Ag_3PO_4(2).

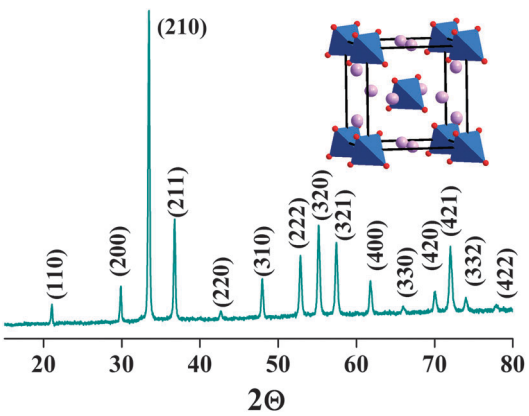

Fig. 2 Powder XRD pattern and the crystal structure (shown in inset) of Ag_3PO_4(1). PO_4 tetrahedron: blue; Ag: violet; O: red.

calculated to be 2.24 eV and 2.32 eV for Ag_3PO_4(1) and Ag_3PO_4(2), respectively. This indicates that multifaceted morphology of the nanoparticles leads to the narrowing of the band gap.

The narrow band gap of the synthesized materials prompted us to examine them as water oxidation catalysts under visible light irradiation. As described earlier, the main objective of this work was to study non-sacrificial water oxidation under visible light irradiation. First, 10 mg of the catalyst and 2 mL of water (degased) were taken in a reactor by maintaining the temperature at 20 °C. A xenon lamp of 300 W with a cut off filter of 420 nm was used for irradiation and the amount of dissolved oxygen molecules was detected using a Clark electrode. It was observed that both Ag_3PO_4 catalysts were active in oxidizing water to oxygen under visible light irradiation. The amount of oxygen produced in 5 minutes for Ag_3PO_4(1) was 150 μmol L^{-1} *vs.* 90 μmol L^{-1} for Ag_3PO_4(2) as

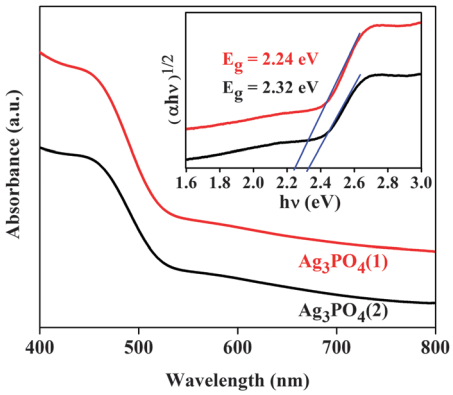

Fig. 3 UV-Vis diffuse reflectance spectra of Ag_3PO_4(1) and Ag_3PO_4(2). Determination of the band gap, $(\alpha h\nu)^{1/2}$ *vs.* $h\nu$, is shown in inset.

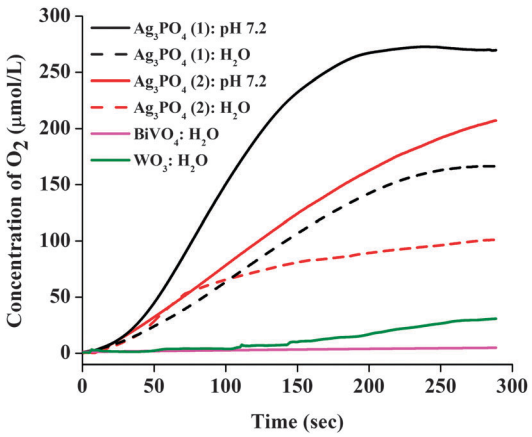

Fig. 4 Visible light driven non-sacrificial water oxidation with multi-faceted Ag_3PO_4(1) and irregular shaped Ag_3PO_4(2) against $BiVO_4$ and WO_3.

shown in Fig. 4. The higher photocatalytic activity of Ag_3PO_4(1) could be explained by the multi-faceted morphology with sharp edges and clear faces and not the surface area, as both Ag_3PO_4(1) (30 $m^2\ g^{-1}$) and Ag_3PO_4(2) (27 $m^2\ g^{-1}$) display similar values. Non-sacrificial water oxidation under similar reaction conditions was also studied for the other two well known $BiVO_4$ and WO_3 photocatalysts. Negligible amounts of oxygen were detected in both cases when irradiated with visible light. This is a remarkable finding proving that Ag_3PO_4 can act as a photocatalyst for non-sacrificial water oxidation. This gives a unique possibility to combine Ag_3PO_4 as the OER part with a hydrogen evolution catalyst for the overall water splitting. It should be noted that OER with Ag_3PO_4 does not require any co-catalysts. However, the main problem associated with this system is the photostability of the catalyst over time which leads to the decrease in activity due to catalyst degradation.

After the successful use of Ag_3PO_4 as the non-sacrificial water oxidation catalyst, we further proceeded to improve the photostability of the catalyst. Bi *et al.* reported that photostability of Ag_3PO_4 particles was increased after AgCl coating.[20] In the present case, the photostability of Ag_3PO_4 could not be increased after the surface coating with AgCl but led to a substantial decrease in photocatalytic activity. Even coating with silica and TiO_2 did not improve the photostability where again significant loss in catalytic activity was observed.

Tremendous enhancement in the photocatalytic activity as well as photostability was observed by changing the reaction medium from water to phosphate buffer (pH = 7.2). Under similar reaction conditions applied for water, 280 μmol L^{-1} of oxygen were produced by Ag_3PO_4(1) whereas Ag_3PO_4(2) produced 210 μmol L^{-1} in phosphate buffer (Fig. 4). We carried out the reactions for a longer period of time and the stability of the catalysts was improved. Re-use of the catalyst for the 2nd and 3rd run was also successfully achieved in phosphate buffer. During water oxidation experiments under visible light irradiation the reduction of Ag_3PO_4 to Ag occurs according to the following equation:[15]

$$4Ag_3PO_4 + 6H_2O + 12\,h + 12\,e \xrightarrow{h\nu} 12Ag + 4H_3PO_4 + 3O_2$$

The higher stability of the catalyst in phosphate buffer could be explained by the presence of excess of phosphate ions which slow down the formation of elemental silver. Powder XRD of Ag_3PO_4(1) after the photochemical experiment (5 minutes) in phosphate buffer did not show any detectable amount of silver formation whereas appearance of Ag reflections could be seen by prolonging the reaction period to 60 minutes (Fig. S3, ESI†). Phosphate buffers with different pH were studied for the water oxidation and it was observed that neutral pH produced the best results. Lower pH decreased the activity whereas a certain increase in activity was observed in basic medium but stability of the catalyst was lost quickly (Fig. 5).

Furthermore, photocatalytic activities of Ag_3PO_4 catalysts have been studied for the degradation of Methyl Blue (MB) dye under visible light irradiation (Fig. S4, ESI†). Both catalysts showed excellent activities in MB degradation as shown in Fig. 6, but the activities of multi-faceted Ag_3PO_4(1) are far better than those of the irregular Ag_3PO_4(2) particles. It should be noted here that a higher concentration of dye and a low amount of catalyst were selected for the studies, to avoid large extent of adsorption of dye on the catalyst surface. MB was completely degraded within 6 minutes with Ag_3PO_4(1) whereas 30 minutes

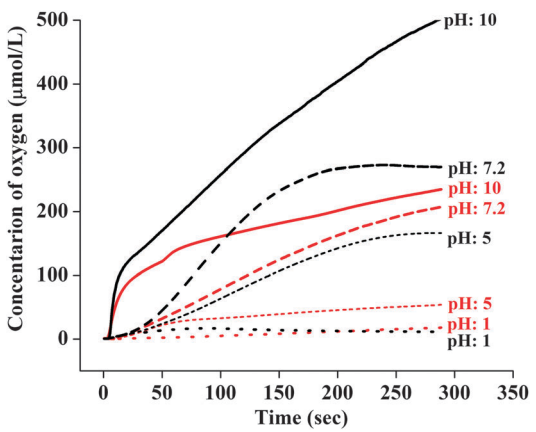

Fig. 5 Visible light driven non-sacrificial water oxidation with Ag_3PO_4(1) and Ag_3PO_4(2) represented in black and red lines, in phosphate buffer at various pH values.

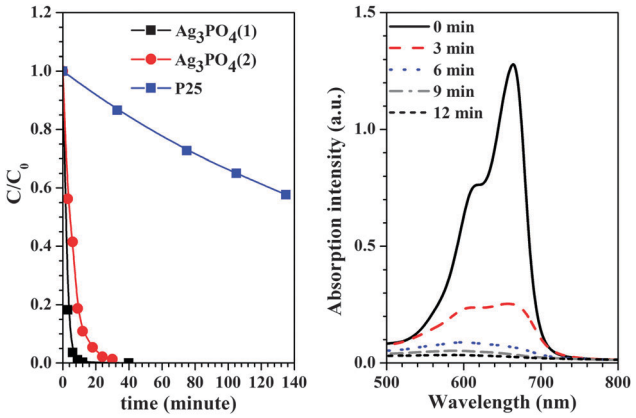

Fig. 6 Variation of the absorbance with time during MB degradation with silver phosphates and P25 (left) and change in concentration of MB with the Ag_3PO_4(1) catalyst (right) under visible light irradiation (>420 nm) at 20 °C.

were required for Ag_3PO_4(2) under visible light irradiation. First, the adsorption of dye was studied on the catalyst surface and a slight decrease in the absorbance was observed after 15 minutes of stirring under dark. Photodegradation of MB with commercially available TiO_2 P25 shows that Ag_3PO_4 are far better catalysts. The MB degradation rate was evaluated based on first order kinetics and the rate constants were found to be 0.50, 0.15 and 0.004 min^{-1} for Ag_3PO_4(1), Ag_3PO_4(2) and P25, respectively. Further, enhancement in the photocatalytic activity of Ag_3PO_4(1) was attributed to the 'clean' faces and sharp edges *vs.* the situation of Ag_3PO_4(2).

In summary, we reported the synthesis and very different activity of multi-faceted *vs.* irregularly shaped silver phosphate particles for the non-sacrificial water oxidation. In phosphate buffer (pH = 7.2), an excellent rate of oxygen evolution was observed with increased photostability under visible light irradiation (>420 nm) at 20 °C. For the photodegradation of Methyl Blue (MB), higher activity of the multi-faceted particles was observed in comparison to the irregular shaped samples. Non-sacrificial water oxidation with multi-faceted silver phosphate particles could lead to overall water splitting by successful coupling of the material with an efficient hydrogen evolution catalyst.

Experimental

Synthesis of Ag_3PO_4(1): in a typical synthesis, 169 mg of $AgNO_3$ was dissolved in 5 mL of water; 5 mL of oleic acid in 5 mL of ethanol was added to the solution and stirred for 10 minutes. Subsequently, 1 mL of phosphoric acid in 5 mL of ethanol was added dropwise to the mixture and stirred for one hour. The yellow solid thus obtained was centrifuged out, washed several times with water and ethanol and dried at 50 °C.

Notes and references

1 (*a*) M. J. Katza, S. C. Riha, N. C. Jeong, A. B. F. Martinson, O. K. Farha and J. T. Hupp, *Coord. Chem. Rev.*, 2012, **256**, 2521–2529; (*b*) M. Kobayashi, S. Masaoka and K. Sakai, *Angew. Chem., Int. Ed.*, 2012, **51**, 7431–7434.
2 (*a*) R. K. Hocking, R. Brimblecombe, L.-Y. Chang, A. Singh, M. H. Cheah, C. Glover, W. H. Casey and L. Spiccia, *Nat. Chem.*, 2011, **3**, 461–466; (*b*) H. Dau and M. Haumann, *Coord. Chem. Rev.*, 2008, **252**, 273–295.
3 (*a*) S. Mukhopadhyay, S. K. Mandal, S. Bhaduri and W. H. Armstrong, *Chem. Rev.*, 2004, **104**, 3981–4026; (*b*) I. Zaharieva, P. Chernev, M. Risch, K. Klingan, M. Kohlhoff, A. Fischer and H. Dau, *Energy Environ. Sci.*, 2012, **5**, 7081–7089.
4 (*a*) M. M. Najafpour, T. Ehrenberg, M. Wiechen and P. Kurz, *Angew. Chem., Int. Ed.*, 2010, **49**, 2233–2237; (*b*) A. Iyer, J. D. Pilar, C. K. Kingondu, E. Kissel, H. F. Garces, H. Huang, M. A. El-Sawy, P. K. Dutta and S. L. Suib, *J. Phys. Chem. C*, 2012, **116**, 6474–6483; (*c*) F. Jiao and H. Frei, *Energy Environ. Sci.*, 2010, **3**, 1018–1027; (*d*) F. Jiao and H. Frei, *Chem. Commun.*, 2010, **46**, 2920–2922.
5 J. Xing, W. Q. Fang, H. J. Zhao and H. G. Yang, *Chem.–Asian J.*, 2012, **7**, 642–657.
6 Y. Sasaki, H. Kato and A. Kudo, *J. Am. Chem. Soc.*, 2013, **135**, 5441–5449.
7 M. Fekete, R. K. Hocking, S. L. Y. Chang, C. Italiano, A. F. Patti, F. Arenae and L. Spiccia, *Energy Environ. Sci.*, 2013, **6**, 2222–2232.
8 (*a*) K. Maeda and K. Domen, *J. Phys. Chem. C*, 2007, **111**, 7851–7861; (*b*) S. S. K. Ma, T. Hisatomi, K. Maeda, Y. Moriya and K. Domen, *J. Am. Chem. Soc.*, 2012, **134**, 19993–19996.
9 Z. Zou, J. Ye, K. Sayama and H. Arakawa, *Nature*, 2001, **414**, 625–627.
10 (*a*) B. Cole, B. Marsen, E. Miller, Y. Yan, B. To, K. Jones and M. Al-Jassim, *J. Phys. Chem. C*, 2008, **112**, 5213–5220; (*b*) B. Cole, B. Marsen, E. Miller, Y. Yan, B. To, K. Jones and M. Al-Jassim, *J. Phys. Chem. C*, 2008, **112**, 5213–5220.
11 S. S. K. Ma, K. Maeda, R. Abe and K. Domen, *Energy Environ. Sci.*, 2012, **5**, 8390–8397.
12 Y. Park, K. J. McDonald and K.-S. Choi, *Chem. Soc. Rev.*, 2013, **42**, 2321–2337.
13 D. K. Zhong, J. Sun, H. Inumaru and D. R. Gamelin, *J. Am. Chem. Soc.*, 2009, **131**, 6086–6087.
14 J. J. Liu, X. L. Fu, S. F. Chen and Y. F. Zhu, *Appl. Phys. Lett.*, 2011, **99**, 191903.
15 Z. Yi, J. Ye, N. Kikugawa, T. Kako, S. Ouyang, H. S. Williams, H. Yang, J. Cao, W. Luo, Z. Li, Y. Liu and R. L. Withers, *Nat. Mater.*, 2010, **9**, 560–564.
16 Y. Bi, H. Hu, S. Ouyang, G. Lu, J. Cao and J. Ye, *Chem. Commun.*, 2012, **48**, 3748–3750.
17 Z. Jiao, Y. Zhang, H. Yu, G. Lu, J. Ye and Y. Bi, *Chem. Commun.*, 2013, **49**, 636–638.
18 Y. Bi, S. Ouyang, N. Umezawa, J. Cao and J. Ye, *J. Am. Chem. Soc.*, 2011, **133**, 6490–6492.
19 S. Kohtani, S. Makino, A. Kudo, K. Tokumura, Y. Ishigaki, T. Matsunaga, O. Nikaido, K. Hayakawa and R. Nakagaki, *Chem. Lett.*, 2002, 660–661.
20 Y. Bi, S. Ouyang, J. Cao and J. Ye, *Phys. Chem. Chem. Phys.*, 2011, **13**, 10071–10075.